

Systolic Elastance and Resistance in the Regulation of Cardiac Pumping Function in Early Streptozotocin-Diabetic Rats

KUO-CHU CHANG,*¹ HUEY-MING LO,[†] AND YUNG-ZU TSENG*[‡]

**Department of Physiology and ‡Department of Internal Medicine, College of Medicine, National Taiwan University, Taipei, Taiwan; and †Department of Medicine, Provincial Tao-Yuan General Hospital, Tao-Yuan, Taiwan*

We determined the roles of maximal systolic elastance (E_{\max}) and theoretical maximum flow (\dot{Q}_{\max}) in the regulation of cardiac pumping function in early streptozotocin (STZ)-diabetic rats. Physically, E_{\max} can reflect the intrinsic contractility of the myocardium as an intact heart, and \dot{Q}_{\max} has an inverse relation to the systolic resistance of the left ventricle. Rats given STZ 65 mg/kg i.v. ($n = 17$) were divided into two groups, 1 week and 4 weeks after induction of diabetes, and compared with untreated age-matched controls ($n = 15$). Left ventricular (LV) pressure and ascending aortic flow signals were recorded to calculate E_{\max} and \dot{Q}_{\max} using the elastance-resistance model. After 1 or 4 weeks, STZ-diabetic animals show an increase in effective LV end-diastolic volume (V_{eed}), no significant change in peak isovolumic pressure (P_{isomax}), and a decline in effective arterial volume elastance (E_a). The maximal systolic elastance E_{\max} is reduced from 751.5 ± 23.1 mmHg/ml in controls to 514.1 ± 22.4 mmHg/ml in 1- and 538.4 ± 33.8 mmHg/ml in 4-week diabetic rats. Since E_{\max} equals $P_{\text{isomax}}/V_{\text{eed}}$, an increase in V_{eed} with unaltered P_{isomax} may primarily act to diminish E_{\max} so that the intrinsic contractility of the diabetic heart is impaired. By contrast, STZ-diabetic rats have higher theoretical maximum flow \dot{Q}_{\max} (40.9 ± 2.8 ml/s in 1- and 44.5 ± 3.8 ml/s in 4-week diabetic rats) than do controls (30.7 ± 1.7 ml/s). There exists an inverse relation between \dot{Q}_{\max} and E_a when a linear regression of \dot{Q}_{\max} on E_a is performed over all animals studied ($r = 0.65$, $p < 0.01$). The enhanced \dot{Q}_{\max} is indicative of the decline in systolic resistance of the diabetic rat heart. The opposing effects of enhanced \dot{Q}_{\max} and reduced E_{\max} may negate each other, and then the cardiac pumping function of the early STZ-diabetic rat heart could be preserved before cardiac failure occurs.

[Exp Biol Med Vol. 227(4):251–259, 2002]

Key words: streptozotocin-diabetic rats; cardiac systolic mechanics; maximal systolic elastance; theoretical maximum flow; effective arterial volume elastance

This study was supported by grants from the National Science Council of Taiwan (nos. NSC 87-2314-B-002-274 and NSC 88-2314-B002-209).

¹ To whom requests for reprints should be addressed at Department of Physiology, College of Medicine, National Taiwan University, No. 1, Sec. 1, Jen-Ai Road, Taipei, Taiwan. E-mail: kechang@ha.mc.ntu.edu.tw

Received February 1, 2001.

Accepted December 12, 2001.

1535-3702/02/2274-0251\$15.00

Copyright © 2002 by the Society for Experimental Biology and Medicine

Diabetes mellitus is a major health problem, and diabetes-induced cardiovascular disease contributes significantly to morbidity and mortality in the diabetic population. In addition to the increased incidence of coronary artery disease and autonomic neuropathy, diabetes mellitus has proven to be an independent risk factor for myocardial dysfunction (1, 2). Many reports in the literature have shown that abnormalities in insulin regulation in streptozotocin (STZ)-diabetic rats may cause disturbances in calcium homeostasis as well as myosin isoenzyme profile (3–7). In the diabetic heart, myocardial dysfunction is associated with abnormalities in the sarcoplasmic reticular and sarcolemmal Ca^{2+} transport and with a depression in the adenosine triphosphatase (ATPase) activities of contractile proteins. Such changes in the cellular physiology of the diabetic heart may be responsible for the mechanical defects that accompany a decline in force generation and a depression in velocity of shortening (8, 9).

The effects of alterations in calcium metabolism and biochemical process on cardiac mechanics can be quantified by making use of the elastance-resistance model (10, 11). The concept of internal resistance on the ventricular pressure-volume relationship is in an attempt to make the elastance model more consistent with the reality of the dynamics of ventricular ejection. Parameters generated by the elastance-resistance model to characterize the systolic pumping mechanics of the left ventricle are E_{\max} and \dot{Q}_{\max} ; E_{\max} is the maximal systolic elastance; \dot{Q}_{\max} is the theoretical maximum flow. In the simplest way, the myocardial contractility could be defined as the “potential to do work” that could reflect the aggregate effects of all mechanisms controlling the activity of the contractile proteins. Any attempt to characterize the myocardial contractility must take into account the ability of the muscle to develop tension and to shorten, which can vary independently of each other, as well as the rate of onset, overall duration, and the decay of both of these variables. E_{\max} is considered the elasticity most sensitive to changes in contractile state and independent of preload, afterload, and heart rate in a given contractile state

of the ventricle (12, 13). These support the view that E_{\max} serves in a given heart to quantify the myocardial contractility of the left ventricle (14).

The quantity in \dot{Q}_{\max} is the amount of outflow generated by the ventricle if it were to eject under zero load condition, and it is inversely related to the ventricular internal resistance (11, 15). An inverse relationship between \dot{Q}_{\max} and percentage of slow myosin ATPase activity has been observed, suggesting that isomyosin composition may be one of the determinants of ventricular resistive behavior (16). Moreover, \dot{Q}_{\max} has also proven to be sensitive to changes in effective arterial volume elastance (E_a) that is derived from left ventricular (LV) end-systolic pressure and stroke volume (17, 18). Thus, the systolic elastance and resistance could describe two independent facets of the LV as a mechanical pump.

Although the effects of diabetes on cardiac mechanics in rats, even in rats with early development of diabetes, have been documented (7, 8, 19, 20), the systolic mechanical behavior of the ventricular pump has never been explored in terms of the systolic elastance and resistance. We hypothesized that changes in specific cardiac proteins and calcium metabolism in diabetes might be associated with impairments in cardiac systolic mechanics in terms of E_{\max} and \dot{Q}_{\max} . Therefore, the goal of the current study was to examine how great the effects of diabetes are on those E_{\max} and \dot{Q}_{\max} in rats with diabetes and their relations in the regulation of systolic performance in early STZ-diabetic rats. We also treated a group of diabetic rats with insulin to establish whether changes in cardiac systolic mechanics were reversible. The novelty of this study is that one can distinguish the effect of \dot{Q}_{\max} from that of E_{\max} on the pumping function of an early STZ-diabetic rat heart.

Materials and Methods

Experimental Preparations. Male Wistar rats weighing 200–250 g at the age of 2 months were used to induce diabetes mellitus in this study. Diabetic rats were induced by a single tail vein injection of STZ at a dose of 65 mg/kg (Sigma Chemical Co., St. Louis, MO). STZ was dissolved in 0.1 M citrate buffer (pH 4.5). Control rats were given an intravenous injection of the vehicle. Forty-eight hours after the injection, induction of diabetes in the STZ-injected rat was confirmed by positive urine glucose using Ames Keto-Diastix (Miles Inc., Elkhart, IN). Untreated diabetic rats were divided into two groups: Group I, 1 week after induction of diabetes ($n = 9$) and Group II, 4 weeks after induction of diabetes ($n = 8$). Animals after induction of diabetes were treated daily with subcutaneous injections of insulin (Novo Nordisk A/S, Bagsvaerd, Denmark) for 4 weeks, and are referred to as Group III ($n = 8$). Urine glucose tests were carried out weekly, and insulin doses were adjusted to maintain negative urine glucose levels (21). The initial insulin doses were 2 U/day, and the largest were 6 U/day at the end of the experimental period. Untreated, age-matched rats ($n = 15$) served as the control group.

All data collected from STZ-diabetic rats were compared with those of untreated controls. The animal experiments were conducted according to the "Guide for the Care and Use of Laboratory Animals", and were approved by the Laboratory Animal Care Committee of the National Taiwan University.

Measurements of Hemodynamic Data. Each rat was intraperitoneally anesthetized with pentobarbital sodium (35 mg/kg). Tracheotomy was performed to provide artificial ventilation with a tidal volume of 5–6 ml/kg and a respiratory rate of 50–70 breaths/min. The chest was opened through the right second intercostal space. An electromagnetic flow probe (model 100 series, internal circumference 8–10 mm; Carolina Medical Electronics, King, NC) was positioned around the ascending aorta to measure the pulsatile aortic flow. A Millar catheter with a high-fidelity pressure sensor (model SPC 320, size 2F; Millar Instruments, Houston, TX) was used to measure the pulsatile pressure waves. Before insertion, the pressure sensor was prewarmed in 37°C saline for at least 1 hr. The catheter was inserted via the isolated right carotid artery into the ascending aorta to measure aortic pressure, and was then moved into the LV to record LV pressure. Total peripheral resistance of the systemic circulation (R_p) was calculated as mean aortic pressure (AoP_m) divided by cardiac output (CO). After being withdrawn from each rat, the catheter was reimmersed in the bath to check for baseline drift. At the end of the experiment, the pressure reading from the sensor submerged in the saline of less than 10 mm in depth was used as the zero pressure reference. The electrocardiogram (ECG) of lead II was recorded with a Gould ECG/Biotach amplifier (Gould Electronics, Cleveland, OH).

The analogue waveforms were sampled at 500 Hz using a 12-bit simultaneously sampling analog-to-digital (A/D) converter interfaced to a personal computer. Selection of signals of 5–10 beats at steady state was made on the basis of the following criteria: i) recorded beats with optimal velocity profile that was characterized by a steady diastolic level, maximal systolic amplitude, and minimal late systolic negative flow; ii) beats with an RR interval (cardiac cycle length) less than 5% different from the average value for all recorded beats; and iii) exclusion of ectopic and postectopic beats. The selective beats were averaged in the time domain using the peak R wave of ECG as a fiducial point. The resulting LV pressure and ascending aortic flow signals were subjected to further analysis using the procedure previously reported (17, 18, 22). First, the isovolumic pressure curve was obtained from the instantaneous pressure of an ejection contraction by a curve-fitting technique. Next, the elastance-resistance model with the estimated isovolumic pressure was applied to measure the systolic mechanical behavior of the ventricular pump.

Estimation of the Isovolumic Pressure from an Ejecting Contraction. To estimate the isovolumic pressure curve $\hat{P}_{iso}(t)$ from an ejecting beat, a nonlinear least-squares approximation technique developed by Sunagawa and colleagues (23) was used:

$$\hat{P}_{iso}(t) = \frac{1}{2} P_{idmax} [1 - \cos(\omega t + c)] + P_d \quad (1)$$

where P_{idmax} is an estimated peak isovolumic developed pressure, ω is an angular frequency, c is a phase shift angle of the sinusoidal curve, and P_d is the LV end-diastolic pressure. The parameter \hat{P}_{isomax} is the estimated peak isovolumic pressure that is the sum of P_{idmax} and P_d . $\hat{P}_{iso}(t)$ is obtained by fitting the measured LV pressure curve segments from the end-diastolic pressure point to the peak positive dP/dt and from the pressure point of the peak negative dP/dt to the same level as the end-diastolic pressure of the preceding beat (24). The peak of the ECG R wave is used to identify the LV end-diastolic point. The upper panel of Figure 1 schematically represents the relation between the ejection contraction and the estimated isovolumic contraction in the pressure-time diagram.

tion contraction and the estimated isovolumic contraction in the pressure-time diagram.

Prediction of the LV Pressure Using an Elastance-Resistance Model. Model-derived pressure of the LV $\hat{P}(t)$ can be calculated by using the elastance-resistance model if the model parameters are previously identified (25, 26). The relationship between instantaneous LV pressure, flow, and isovolumic pressure can be written as follows:

$$\hat{P}(t) = P_{iso}(t) \left[1 - \frac{V_{ej}(t)}{V_{eed}} \right] \left[1 - \frac{\dot{Q}(t)}{\dot{Q}_{max}} \right] \quad (2)$$

where $V_{ej}(t)$ is instantaneously ejected volume computed by numerically calculating the running integral of the aortic flow signal $\dot{Q}(t)$. \dot{Q}_{max} is the theoretical maximum flow (i.e., the amount of outflow generated by the ventricle if it were to eject under zero load condition). V_{eed} is an effective LV end-diastolic volume that is the volume difference between LV end-diastolic volume (V_{ed}) and the zero-pressure volume axis intercept (V_0). $P_{iso}(t)$ is the isovolumic pressure obtained by occluding the ascending aorta near the sinuses of Valsalva at the end of diastole. Herein, $P_{iso}(t)$ is replaced with $\hat{P}_{iso}(t)$ that is derived from the measured pressure of an ejecting contraction by making use of Equation 1.

Both V_{eed} and \dot{Q}_{max} are the model parameters that remain to be determined by curve-fitting techniques. Campbell and colleagues (10) found that Equation 2 can be used to fit the measured LV pressure of an ejecting beat very well, if the fitting interval is $t_{ej} < t < t_{pisomax}$, where t_{ej} is the onset of ventricular ejection and $t_{pisomax}$ is the time of peak isovolumic pressure. The normalized root-mean-square e_p is

$$e_p = \frac{1}{n} \sqrt{\sum_{i=1}^n \frac{[P(i) - \hat{P}(i)]^2}{\bar{P}}} \quad (3)$$

where $P(i)$ and $\hat{P}(i)$ are the sampled values of observed and model-calculated pressure of the LV, respectively. Initial values of the parameters, V_{eed} and \dot{Q}_{max} , are chosen first. The Nelder-Mead simplex algorithm (27) is then used to iteratively adjust V_{eed} and \dot{Q}_{max} to minimize the normalized root-mean-square value. The parameters coincident with the minimum objective function are taken as the model estimates of the systolic pumping mechanics of the LV. The LV systolic elastance $E(t)$ can be calculated by the formulation of $E(t) = \hat{P}_{iso}(t)/V_{eed}$. The maximal systolic elastance E_{max} is, therefore, quantified in terms of its maximal value, $E_{max} = P_{isomax}/V_{eed}$ and the internal resistance R in terms of the theoretical maximum flow \dot{Q}_{max} , $R(\hat{P}_{iso}) = \hat{P}_{iso}(t)/\dot{Q}_{max}$.

Fitness of the data generated by the model is judged by the magnitude of e_p and by indices from a linear regression of the model-generated pressure $\hat{P}(i)$ on the measured pressure $P(i)$. Two indices are used to evaluate the goodness-of-fit: the coefficient of determination, r^2 , and the standard error of the estimate, SEE . We look for r^2 to be close to 1 and for SEE to be on the order of less than 5% when ex-

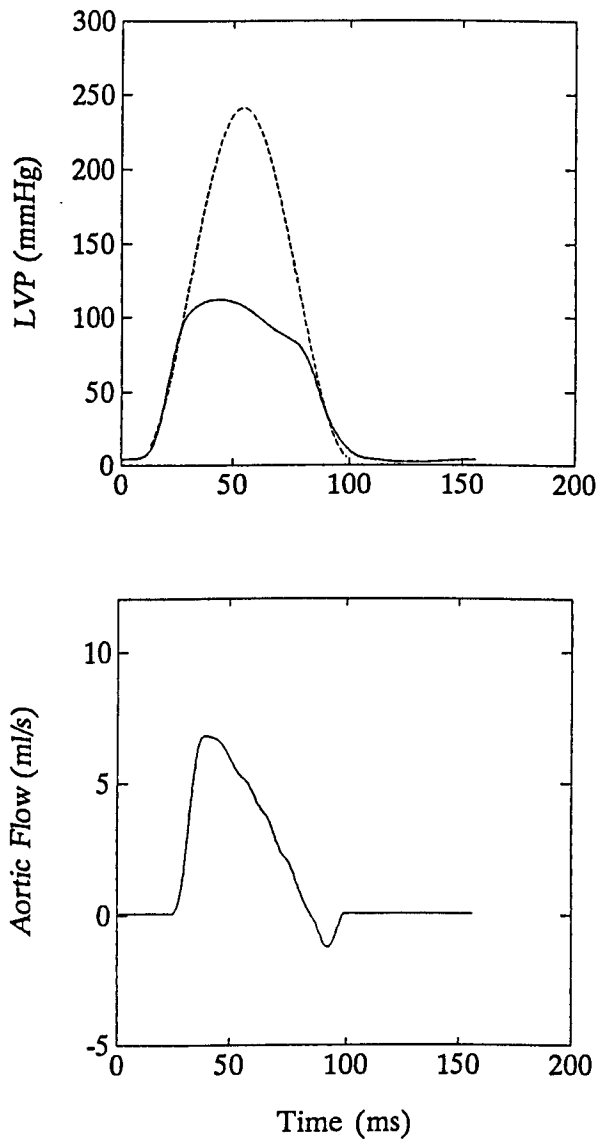


Figure 1. The solid curves show the measured LV pressure waveform (upper panel) and ascending aortic flow signal (lower panel) in a control rat. In the upper panel, the dashed line represents the isovolumic pressure curve at an end-diastolic volume, which is estimated by fitting a sinusoidal function to the isovolumic portions of the measured LV pressure.

pressed relative to the mean of pressure observations (28). Figure 2 shows the similarity between the computed and measured pressure waveforms during the fitting interval $t_{ej} < t < t_{pisomax}$.

Effective Arterial Volume Elastance as Arterial Chamber Property. The effective arterial volume elastance (E_a) could be calculated as follows. The peak isovolumic pressure of the LV at the end-diastolic volume is estimated by Equation 1. The pressure-ejected volume loop can be obtained by the time integration of aortic flow and the measured LV pressure (Fig. 3). Drawing a tangential line from the estimated peak isovolumic pressure to the right corner of the pressure-ejected volume loop yields a point referred to as end-systolic equilibrium point (29). The pressure of the LV at this end-systolic equilibrium point is the LV end-systolic pressure. Thus, the slope of the end-systolic pressure versus stroke volume relation (i.e., P_{es}/SV ; the dashed in Fig. 3) represents the effective arterial volume elastance E_a (30).

Statistics. Results are expressed as means \pm SE. No differences in all hemodynamic parameters studied were observed between 1- and 4-week control rats, and then all control data were consolidated. Differences between the three diabetic and control groups were detected using one-way analysis of variance (ANOVA). Where differences were found, significance was determined with Dunnett's test for multiple comparisons with a single control. Statistical significance is defined at the level of $P < 0.05$.

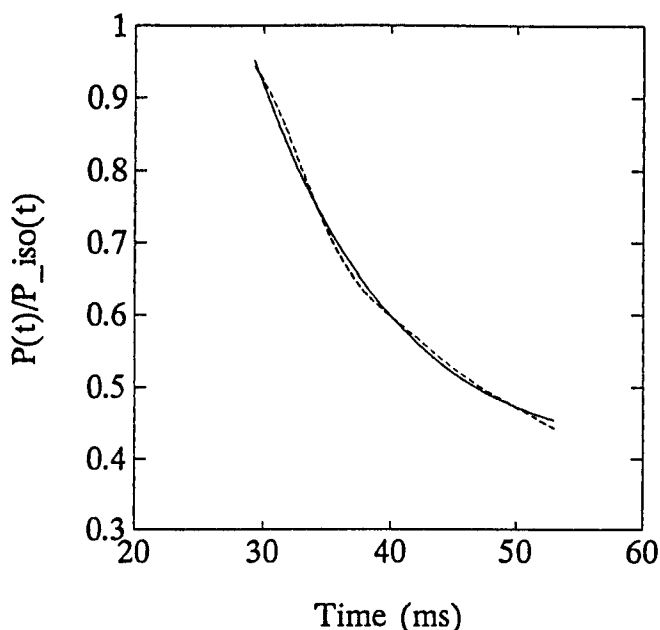


Figure 2. The measured data (solid line) and model-generated data (dashed line) when the elastance-resistance model is fitted over $t_{ej} < t < t_{pisomax}$. Little distinction can be made between the model-generated and observed data. The LV pressure is normalized to the estimated isovolumic pressure.

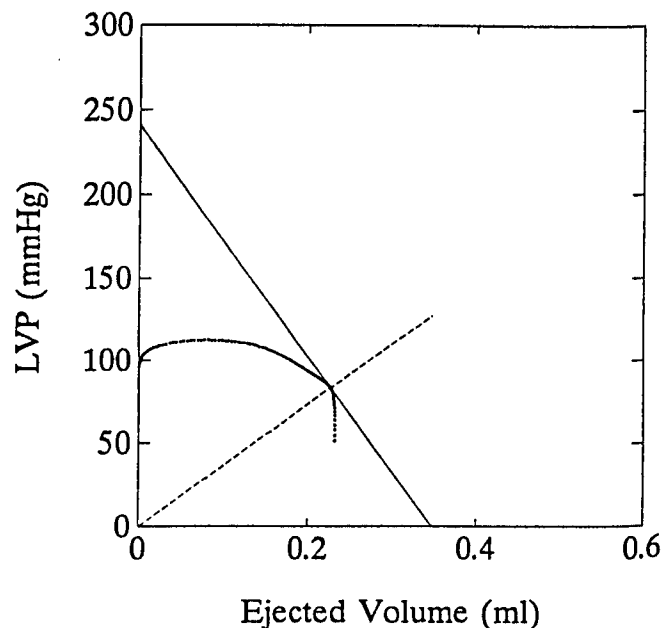


Figure 3. Drawing a tangential line from the estimated peak isovolumic pressure to the right corner of the pressure-ejected volume loop yields a point referred to as the end-systolic equilibrium point. The pressure of the left ventricle at this point is the LV end-systolic pressure (P_{es}). The slope of the dashed line connecting the end-diastolic point to the end-systolic equilibrium point represents the effective arterial volume elastance (E_a).

Results

As expected, after the β cell of the islet of Langerhans was destroyed by STZ, STZ treatment to rats resulted in consistent hyperglycemia that persisted over the period of the experiment. In addition, STZ-diabetic rats had lower body weights and LV weights when compared with controls (Table I).

The effects of diabetes on basic hemodynamic variables and arterial chamber properties are shown in Figures 4 and 5. After 1 or 4 weeks, insulin-deficient diabetic rats had decreased basal heart rate (HR in Fig. 4A), and increased cardiac output (CO in Fig. 4B), as well as stroke volume (SV in Fig. 4C). There was no significant change in mean aortic pressure (AoP_m in Fig. 5A), whereas a decline in total peripheral resistance (R_p in Fig. 5B) was observed in STZ-diabetic rats. As for the chamber properties of the arterial system, animals with insulin deficiency showed a significant fall in E_a (Fig. 5C).

The results of fitting the elastance-resistance model to LV pressure showed little distinction between the model-generated and measured signals. The averaged values for e_p as an indication of the quality of fit was 0.0032 ± 0.0001 , for r^2 was 0.9850 ± 0.0021 , and for SEE was $2.68\% \pm 0.17\%$. These results indicate that the model parameters were estimated with good quality in analyzing the cardiac systolic mechanics with the elastance-resistance model.

Figures 6 and 7 depict the effects of diabetes on cardiac systolic mechanical behavior that is characterized by E_{max}

Table I. Body and Heart Weight and Glucose Levels in Control and STZ-Induced Diabetic Rats

	NC (n = 15)	DM 1 week (n = 9)	DM 4 weeks (n = 8)	DM + INSULIN (n = 8)
Body weight (g)	335.6 ± 18.9	278.9 ± 12.4 ^a	271.3 ± 6.1 ^b	347.5 ± 9.2
LV weight (mg)	690.4 ± 29.5	588.8 ± 30.4 ^a	577.8 ± 12.9 ^b	699.1 ± 12.2
Glucose (mg/dl)	128.1 ± 8.5	416.7 ± 19.4 ^b	457.6 ± 10.2 ^b	217.1 ± 14.4 ^b

Note. All values are expressed as means ± SE. No differences in body weight, LV weight, and blood sugar were observed between 1- and 4-week control rats, and then all control data were consolidated. All data collected from STZ-diabetic rats were compared with those of untreated controls. NC, age-matched controls; DM, STZ-diabetic rats; DM + INSULIN, insulin-treated rats of diabetes.

^a $P < 0.05$ compared with controls.

^b $P < 0.01$ compared with controls.

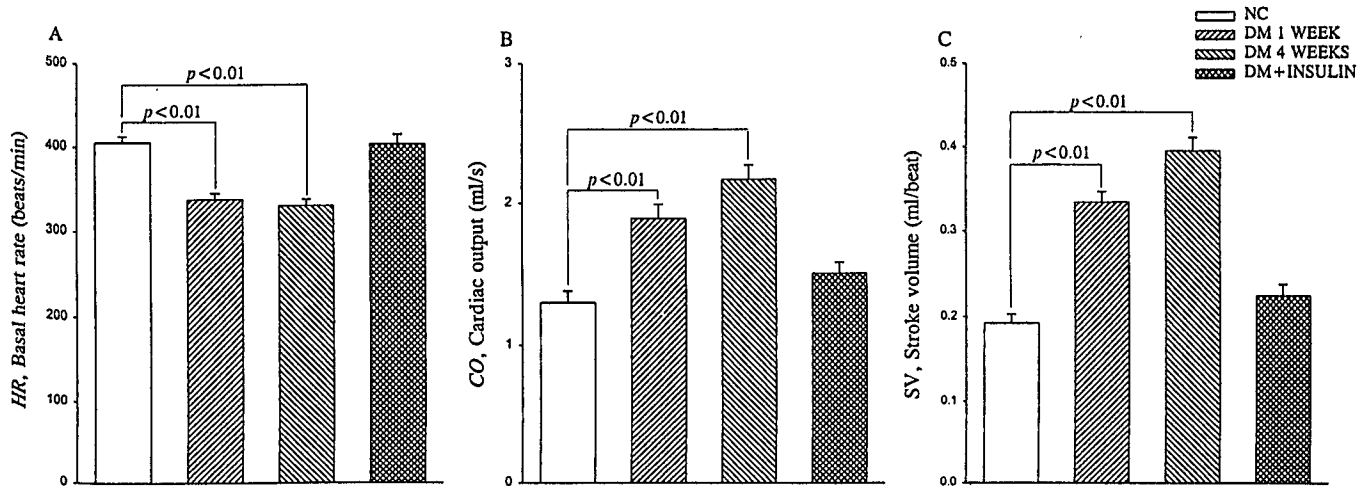


Figure 4. Effects of diabetes on basal heart rate, cardiac output, and stroke volume. All values are expressed as means ± SE. No differences in HR, CO and SV were observed between 1- and 4-week control rats and then all control data were consolidated. All data collected from STZ-diabetic rats were compared with those of untreated controls. Insulin-deficient diabetic rats had decreased HR (A), and increased CO (B) as well as SV (C). The diabetes-related changes in HR, CO, and SV could be prevented by the treatment with insulin. NC, age-matched controls; DM, STZ-diabetic rats; DM + INSULIN, insulin-treated rats of diabetes.

and \dot{Q}_{\max} . Neither LV end-systolic pressure (P_{es} in Fig. 6A) nor estimated peak isovolumic pressure (P_{isomax} in Fig. 6B) was affected by diabetes after 1 or 4 weeks of injection of STZ. However, the amount of V_{eed} (Fig. 6C) in insulin-deficient diabetic hearts was much greater than that in control, nondiabetic hearts. Since E_{\max} is determined by the ratio of P_{isomax} to V_{eed} , STZ-diabetic rats had lower E_{\max} (514.1 ± 22.4 mm Hg/ml in 1-week diabetic rats and 538.4 ± 33.8 mm Hg/ml in 4-week diabetic rats) than did controls (751.5 ± 23.1 mm Hg/ml), shown in Figure 7A. When normalized for LV weight, E_{\max} of the diabetic heart (i.e., $E_{\max n} = E_{\max}/LV$ weight in Fig. 7B) was still significantly lower than that of the control heart. By contrast, STZ-diabetic rats had higher \dot{Q}_{\max} (40.9 ± 2.8 ml/sec in 1-week diabetic rats and 44.5 ± 3.8 ml/sec in 4-week diabetic rats) than did controls (30.7 ± 1.7 ml/sec), shown in Figure 7C. There was an inverse relation between \dot{Q}_{\max} and E_a when a linear regression of \dot{Q}_{\max} on E_a was performed over all animals studied ($r = 0.65$, $P < 0.001$; Fig. 8).

Administration of insulin to STZ-diabetic rats resulted in weight gains and lowering of serum glucose (Table I). All basic hemodynamic variables returned to baseline after a 4-week treatment with insulin (Figs. 4 and 5). Furthermore,

insulin treatment had apparent effect on the systolic mechanical behavior of the ventricular pump as measured by V_{eed} (Fig. 6C), E_{\max} (Fig. 7A), and \dot{Q}_{\max} (Fig. 7C).

Discussion

The most striking findings of this study are that there is an increase in \dot{Q}_{\max} and a decrease in E_{\max} in the early STZ-diabetic rat heart. The opposing effects of enhanced \dot{Q}_{\max} and reduced E_{\max} may negate each other, and thus the cardiac pumping function of the early STZ-diabetic rat could be preserved before cardiac failure occurs.

Effects of Diabetes on the Contractile Status of the LV. As mentioned earlier, both the peak isovolumic pressure P_{isomax} and the effective LV end-diastolic volume V_{eed} determine the maximal systolic elastance E_{\max} that equals P_{isomax}/V_{eed} . Because no alteration is noticed in P_{isomax} , a significant rise in V_{eed} may primarily act to diminish E_{\max} in the early STZ-diabetic rat heart. This result implies that the diabetic myocardium is incapable of producing the pressure force enough to support E_{\max} along with the increased V_{eed} . Thus, an increase in V_{eed} with unchanged P_{isomax} suggests that some defects in the myofilament sys-

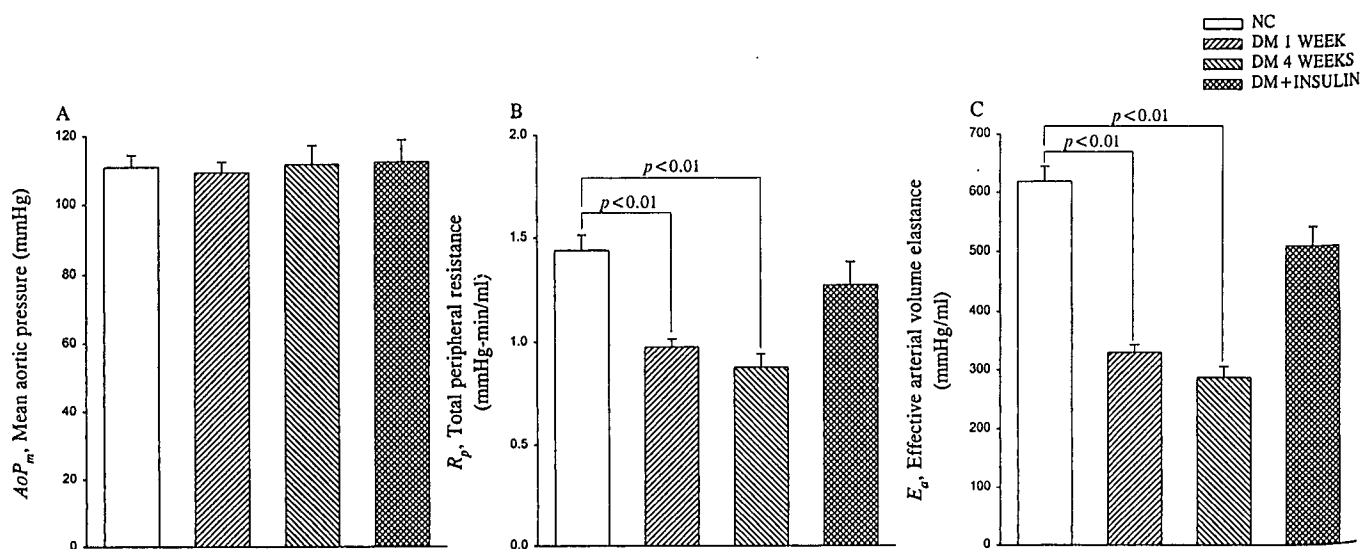


Figure 5. Effects of diabetes on mean aortic pressure, total peripheral resistance, and effective arterial volume elastance. All values are expressed as means \pm SE. No differences in AoP_m , R_p and E_a were observed between 1- and 4-week control rats and then all control data were consolidated. All data collected from STZ-diabetic rats were compared with those of untreated controls. Although no significant change was seen in AoP_m (A), STZ-diabetic rats showed a decline in R_p (B) and E_a (C). The diabetes-related changes in R_p and E_a could be prevented by insulin therapy. NC, age-matched controls; DM, STZ-diabetic rats; DM + INSULIN, insulin-treated rats of diabetes.

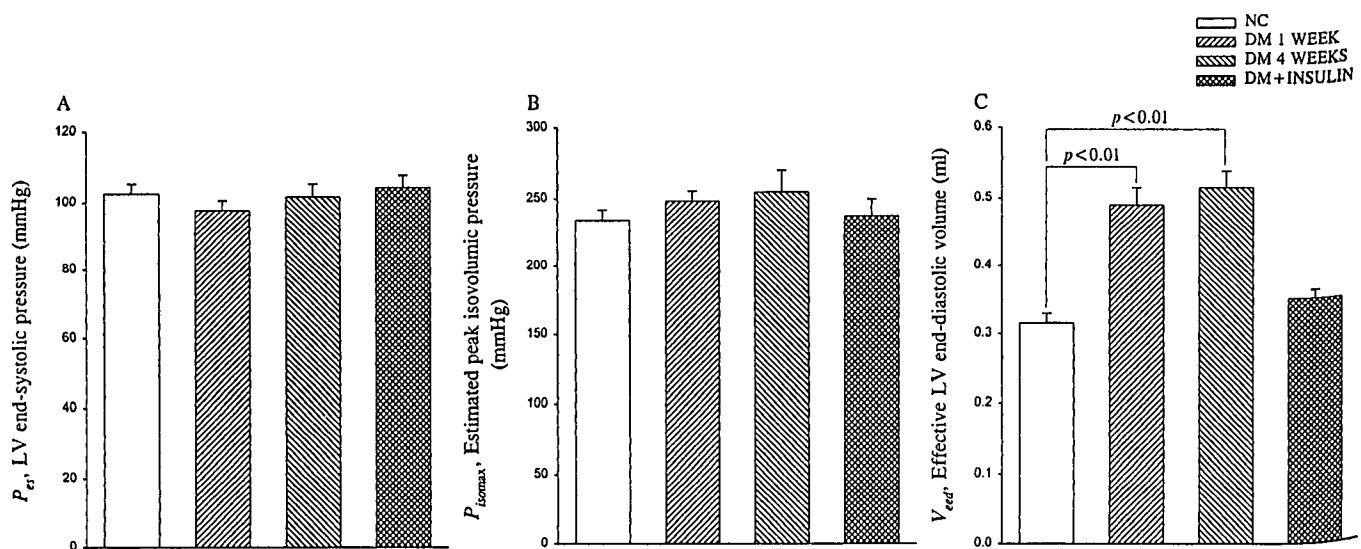


Figure 6. Effects of diabetes on LV end-systolic pressure, estimated peak isovolumic pressure, and effective LV end-diastolic volume. All values are expressed as means \pm SE. No differences in P_{es} , P_{isomax} , and V_{eed} were observed between 1- and 4-week control rats and then all control data were consolidated. All data collected from STZ-diabetic rats were compared with those of untreated controls. Although no significant changes were seen in P_{es} (A) and P_{isomax} (B), STZ-diabetic heart exhibited an increase in V_{eed} (C). The diabetes-related change in V_{eed} could be prevented by the treatment with insulin. NC, age-matched controls; DM, STZ-diabetic rats; DM + INSULIN, insulin-treated rats of diabetes.

tems may occur in the early STZ-diabetic rat heart. It has been suggested that the properties of the contractile unit, along with the activation process (i.e., availability of Ca^{2+}), may determine the elastic behavior of the ventricle (11, 12). The impaired contractile status of the diabetic heart could be related to abnormalities in calcium metabolism due to defects in the sarcolemmal Na^+-Ca^{2+} exchange (31) and the Ca^{2+} uptake of sarcoplasmic reticulum (7, 32). Therefore, alterations in calcium homeostasis or other factors in the myofilament systems to worsen the P_{isomax} - V_{eed} relation may profoundly affect E_{max} , deteriorating the intrinsic contractility of the early STZ-diabetic rat heart.

Effects of Diabetes on the Systolic Resistance of the LV. Change that takes place in another aspect of cardiac mechanics with diabetes is an increase in theoretical maximum flow \dot{Q}_{max} . Many reports in the literature demonstrated the occurrence in the diabetic myocardium of the shift of the myosin isoenzyme profile from the fast V_1 isoform toward the slow V_3 isoform (3, 6, 7). One would expect that this isoenzyme shift in the diabetic myocardium might cause a decline in \dot{Q}_{max} because of the inverse relation between \dot{Q}_{max} and percent slow V_3 isoform (16). By contrast, we show data quite different from that speculation based on the biochemical changes in the diabetic heart. That

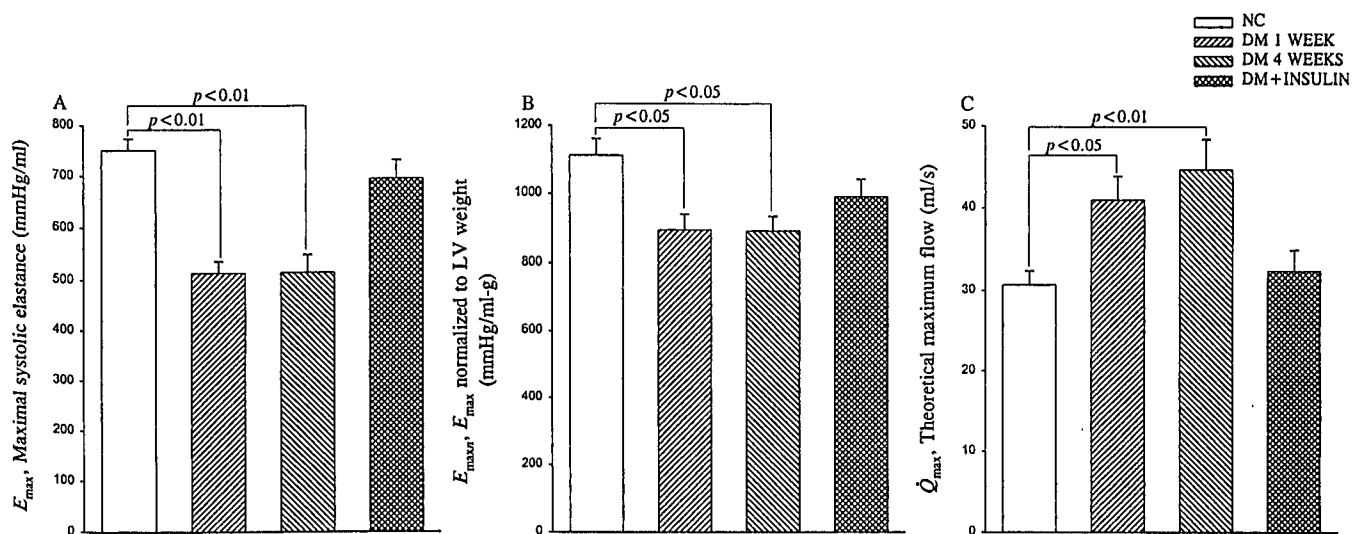


Figure 7. Effects of diabetes on maximal systolic elastance and theoretical maximum flow. All values are expressed as means \pm SE. No differences in E_{max} and \dot{Q}_{max} were observed between 1- and 4-week control rats and then all control data were consolidated. All data collected from STZ-diabetic rats were compared with those of untreated controls. There was a decline in E_{max} in insulin-deficient diabetic heart (A). To account for differences in LV mass by diabetes, E_{max} was normalized by dividing with LV weight (i.e., $E_{max,n} = E_{max}/LV \text{ weight}$). The LV intrinsic contractility was depressed in diabetic rats, as evidenced by the reduced $E_{max,n}$ (B). On the contrary, \dot{Q}_{max} exhibited a significant rise in the diabetic heart (C), suggesting a fall in LV systolic resistance. Diabetes-related changes in E_{max} , $E_{max,n}$, and \dot{Q}_{max} could be prevented by insulin therapy. NC, age-matched controls; DM, STZ-diabetic rats; DM + INSULIN, insulin-treated rats of diabetes.

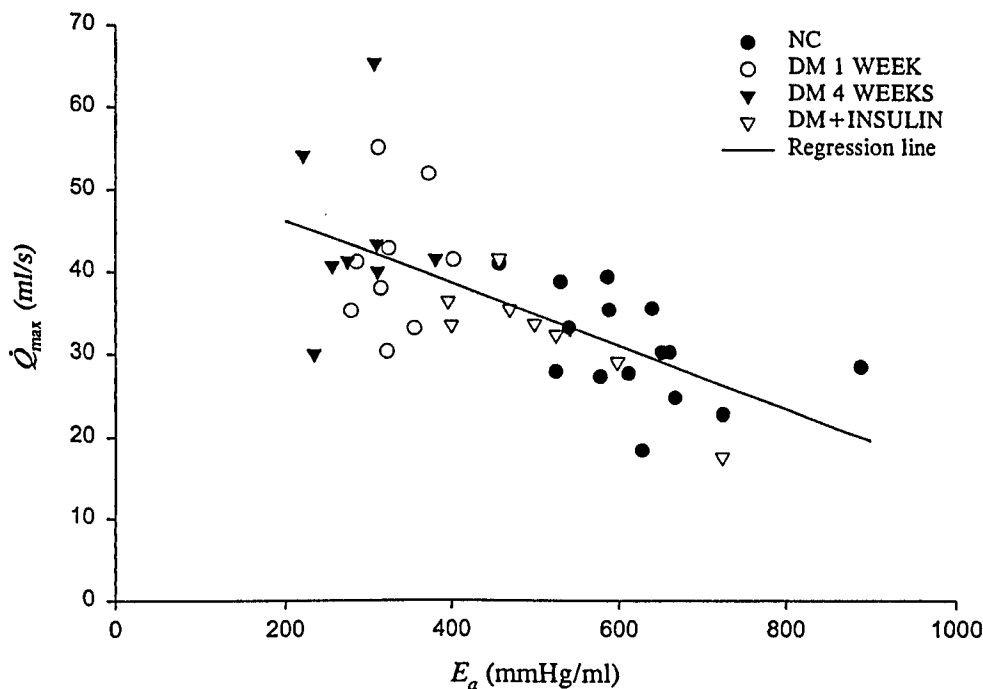


Figure 8. Theoretical maximum flow \dot{Q}_{max} plotted against effective arterial volume elastance E_a . No significant relation between \dot{Q}_{max} and E_a was observed within each group ($P > 0.05$). However, an inverse relation between \dot{Q}_{max} and E_a is evident after pooling the data of all groups. The solid line is obtained when a linear regression of \dot{Q}_{max} on E_a is performed over all animals studied, having the linear equation $\dot{Q}_{max} = 53.833 - 0.038 \times E_a$ with $r = 0.65$; $P < 0.001$.

is because arterial chamber properties also play an important role in determining \dot{Q}_{max} (17, 18, 26). In this study, either 1- or 4-week STZ-diabetic rats exhibited a decline in basal heart rate HR and a fall in total peripheral resistance R_p . Because the effective arterial volume elastance E_a can be reasonably approximated by the ratio of physical resistance to cardiac cycle length (30), the diminished R_p and HR accounts for the reduction in E_a in diabetes. There existed an inverse relation between \dot{Q}_{max} and E_a when a linear regression of \dot{Q}_{max} on E_a was performed over all animals

studied ($r = 0.65$, $P < 0.01$; Fig. 8). Our data suggest that the diabetes-related decline in E_a , but not the changes in myosin ATPase activity, may be the major factor responsible for the increase in \dot{Q}_{max} in early diabetes. The enhanced \dot{Q}_{max} is indicative of the decline in ventricular internal resistance of the STZ-diabetic rat heart.

Ventricular-Arterial Coupling in STZ-Diabetic Rats. It has been suggested that the equilibrium stroke volume SV is directly proportional to both V_{eed} and E_{max} and is inversely related to R_p (30). The ventricular systolic re-

sistance may also affect performance of the LV under pathological states (11, 25). In this study, the STZ-diabetic rat exhibited a decline in R_p and a fall in ventricular systolic resistance to enhance SV . Ventricular dilatation, as defined by an increase in V_{eed} , also developed in the diabetic heart to increase SV . Thus, despite lower basal heart rate and depressed cardiac contractility, STZ-diabetic rats are able to enhance stroke volume, causing an increase in blood flow and maintaining blood pressure as seen in controls. Our data suggest that at the early stage of the STZ-diabetic rat heart, the opposing effects of augmented \dot{Q}_{max} and reduced E_{max} may negate each other, and then the pumping function of the diabetic heart could be preserved before cardiac failure occurs.

Effects of Insulin Administration to STZ-Diabetic Rats. In this study, insulin therapy may correct V_{eed} but maintain P_{isomax} so that the contractile status of the early STZ-diabetic rat heart could be prevented. The administration of insulin to diabetic animals may stimulate the sarcolemmal $Na^+-K^+-ATPase$ activity (33) and Na^+-Ca^{2+} exchange in cardiac muscle cells (34), and then result in calcium homeostasis. Those contribute to the return of the impaired intrinsic contractility of the diabetic heart to baseline, as manifested by the regressed E_{max} . Either HR or R_p or E_a was also reversed by the administration of insulin to STZ-diabetic rats. On the other hand, the normalized \dot{Q}_{max} by the diabetic control may cause the return of the ventricular internal resistance to baseline. Our data suggest that all abnormalities in cardiac systolic mechanics in the early STZ-diabetic rat heart may be prevented by insulin therapy.

Limitations. Rats treated with STZ display many of the features seen in human subjects with uncontrolled diabetes mellitus, including hyperglycemia, polydipsia, polyuria, and weight loss (35). However, STZ has the potential to affect many factors such as endocrine, renal, hepatic, nervous, cardiac, and vascular factors that may underlie changes in cardiovascular homeostasis. The results reported here were obtained in STZ-diabetic rats, and caution should be noted in extrapolating all findings from STZ-diabetic rats to human subjects with insulin deficiency. More studies on different models of diabetes are needed to delineate the effects of diabetes on the systolic mechanical behavior of the LV in terms of \dot{Q}_{max} and E_{max} .

There is a concern about the estimation of the isovolumic pressure from an ejection beat. Campbell and colleagues (26) demonstrated that the duration of the isovolumic contraction by abruptly clamping the aortic root is significantly longer than that of the ejecting contraction. However, this prolongation was observed mainly at the diastole; during the rising phase, there was an overlap of pressure traces between the isovolumic and ejecting contractions (Fig. 2A in Ref. 26). Moreover, Sunagawa and colleagues (23) showed that the predicted P_{isomax} has good correlation with that obtained by actual aortic occlusion. Because the fitting interval is $t_{ej} < t < t_{pisomax}$, the elastance-

resistance model with the estimated isovolumic pressure could be used to measure E_{max} and \dot{Q}_{max} .

Another concern is that the elastance-resistance model is not a perfect model in the evaluation of the LV systolic mechanics. Hunter and colleagues (12, 36) demonstrated that besides elastance and resistance, there are at least two or more processes involved in the description of systolic mechanical behavior of the ventricular pump. These processes may include the volume influence factor and the deactivation factor. However, Campbell and colleagues (10) showed that the elastance-resistance model could be used to fit the measured LV pressure of an ejection beat very well if the fitting interval is $t_{ej} < t < t_{pisomax}$. Shroff and colleagues (11) believe that the elastance-resistance is a useful model to quantify LV systolic mechanical properties, provided one clearly understands its limitations.

The depressed myocardial effects (37) and the impaired gain of baroreceptor reflex function (38) may be exerted by sodium pentobarbital in rats. Thus, this kind of anesthetic may be not an ideal anesthetic agent for the use of studying cardiovascular dynamics in rats. In this report, the results pertained only to measurements made in the open-chest rat with pentobarbital anesthesia. This setting induced a fall in blood pressure and may introduce reflex effects not found in the closed-chest setting. Just how much pentobarbital anesthesia and thoracotomy affect pulsatile hemodynamics in rats was uncertain. However, studies on other animal models suggest that the effects are small relative to biological and experimental variability between animals (39). More studies are needed to elucidate the differential effects of anesthetics on the systolic mechanical behavior of the LV in terms of \dot{Q}_{max} and E_{max} in rats with diabetes.

In summary, the most striking findings of this study are that there is an increase in \dot{Q}_{max} and a decrease in E_{max} in the early STZ-diabetic rat heart. An increase in V_{eed} with unaltered P_{isomax} may primarily act to diminish E_{max} so that the intrinsic contractility of the diabetic heart is impaired. Moreover, the diabetes-related fall in E_a may be the major factor responsible for the increased \dot{Q}_{max} in diabetes. The enhanced \dot{Q}_{max} is indicative of the decline in ventricular internal resistance of the STZ-diabetic rat. The opposing effects of enhanced \dot{Q}_{max} and reduced E_{max} may negate each other, and thus the pumping function of the early STZ-diabetic rat heart could be preserved before cardiac failure occurs. Our data also suggest that all abnormalities in cardiac systolic mechanics in the early STZ-diabetic rat heart may be prevented by insulin therapy.

1. Kannel WB, Hjortland M, Castelli WP. Role of diabetes in congestive heart failure: the Framingham study. *Diabetes* 34:29-34, 1974.
2. Regan TJ, Lyons MM, Ahmed SS, Levinson GE, Oldewurtel HA, Ahmed MR, Haider B. Evidence for cardiomyopathy in familial diabetes mellitus. *J Clin Invest* 60:885-899, 1977.
3. Dillmann WH. Diabetes mellitus induces changes in cardiac myosin in the rat. *Diabetes* 29:579-582, 1980.
4. Fein FS, Kornstein LB, Strobeck JE, Capasso JM, Sonnenblick EH.

- Altered myocardial mechanics in diabetic rats. *Circ Res* **47**:922–933, 1980.
5. Penpargkul S, Schaibel T, Yiointsoi T, Scheuer J. The effects of diabetes on performance and metabolism of rat hearts. *Circ Res* **47**:911–921, 1980.
 6. Malhotra A, Penpargkul S, Fein FS, Sonnenblick EH, Scheuer J. The effects of streptozotocin-induced diabetes in rats on cardiac contractile proteins. *Circ Res* **49**:1243–1250, 1981.
 7. Penpargkul S, Fein FS, Sonnenblick EH, Scheuer J. Depressed cardiac sarcoplasmic reticular function from diabetic rats. *J Mol Cell Cardiol* **13**:303–309, 1981.
 8. Okayama H, Hamada M, Hiwada K. Contractile dysfunction in the diabetic-rat heart is an intrinsic abnormality of the cardiac myocytes. *Clin Sci* **86**:257–262, 1994.
 9. Yu Z, Tibbitts GF, McNeill JH. Cellular functions of diabetic cardiomyocytes: contractility, rapid-cooling contracture, and ryanodine binding. *Am J Physiol* **266**:H2082–H2089, 1994.
 10. Campbell KB, Ringo JA, Knowlen GG, Kirkpatrick RD, Schmidt SL. Validation of optimal elastance-resistance left ventricle pump models. *Am J Physiol* **251**:H382–H397, 1986.
 11. Shroff SG, Janicki JS, Weber KT. Mechanical and energetic behavior of the intact left ventricle. In: Fozzard HA, Eds. *The Heart and Cardiovascular System*, (2nd ed). New York: Raven Press, pp129–150, 1992.
 12. Hunter WC, Janicki JS, Weber KT, Noordergraaf A. Systolic mechanical properties of the left ventricle: effects of volume and contractile state. *Circ Res* **52**:319–327, 1983.
 13. Suga H, Sagawa K, Shoukas AA. Load independence of the instantaneous pressure-volume ratio of the canine left ventricle and effects of epinephrine and heart rate on the ratio. *Circ Res* **32**:314–322, 1973.
 14. Schertel ER. Assessment of left-ventricular function. *Thorac Cardiovasc Surg* **46**(Suppl.):248–254, 1998.
 15. Shroff SG, Janicki JS, Weber KT. Evidence and quantitation of left ventricular systolic resistance. *Am J Physiol* **249**:H358–H370, 1985.
 16. Shroff SG, Naegelen D, Clark WA. Relation between left ventricular systolic resistance and contractile rate processes. *Am J Physiol* **258**:H381–H394, 1990.
 17. Chang KC. Theoretical maximal flow of the left ventricle is sensitive to change in ventricular afterload. *J Theor Biol* **194**:409–417, 1998.
 18. Chang KC, Peng YI, Dai SH, Tseng YZ. Age-related changes in pumping mechanical behavior of rat ventricle in terms of systolic elastance and resistance. *J Gerontol:BS* **55A**:B440–B447, 2000.
 19. Dowell RT, Atkins FL, Love S. Integrative nature and time course of cardiovascular alterations in the diabetic rat. *J Cardiovasc Pharmacol* **8**:406–413, 1986.
 20. Litwin SE, Raya TE, Anderson PG, Daugherty S, Goldman S. Abnormal cardiac function in the streptozotocin-diabetic rat: changes in active and passive properties of the left ventricle. *J Clin Invest* **86**:481–488, 1990.
 21. Carbonell LF, Salomalom MG, Garcia-Estan J, Salazar FJ, Ubeda M, Quesada T. Hemodynamic alterations in chronically conscious unrestrained diabetic rats. *Am J Physiol* **252**:H900–H905, 1987.
 22. Chang KC, Kuo TS. Single-beat estimation of the ventricular pumping mechanics in terms of the systolic elastance and resistance. *J Theor Biol* **189**:89–95, 1997.
 23. Sunagawa K, Yamada A, Senda Y, Kikuchi Y, Nakamura M, Shibahara T, Nose Y. Estimation of the hydromotive source pressure from ejection beats of the left ventricle. *IEEE Trans Biomed Eng* **27**:299–305, 1980.
 24. Takeuchi M, Igarashi Y, Tomimoto S, Odake M, Hayashi T, Tsukamoto T, Hata K, Takaoka H, Fukuzaki H. Single-beat estimation of the slope of the end-systolic pressure-volume relation in the human left ventricle. *Circulation* **83**:202–212, 1991.
 25. Shroff SG, Motz W. Left ventricular systolic resistance in rats with hypertension and hypertrophy. *Am J Physiol* **257**:H386–H394, 1989.
 26. Campbell KB, Kirkpatrick RD, Knowlen GG, Ringo JA. Late-systolic pumping properties of the left ventricle: deviation from elastance-resistance behavior. *Circ Res* **66**:218–233, 1990.
 27. Dennis JE, Woods DJ. New Computing Environments. In: Wouk A, Ed. *Microcomputers in Large-Scale Computing*. Philadelphia: Society for Industrial and Applied Mathematics. pp116–122, 1987.
 28. Draper NR, Smith H. *Applied Regression Analysis* (2nd ed). New York: John Wiley & Sons, pp417, 1981.
 29. Barnea O, Jaron D. A new method for the estimation of the left ventricular pressure-volume area. *IEEE Trans Biomed Eng* **37**:109–111, 1990.
 30. Sunagawa K, Sagawa K, Maughan WL. Ventricular interaction with the loading system. *Ann Biomed Eng* **12**:163–189, 1984.
 31. Makino N, Dhalla KS, Elimban V, Dhalla NS. Sarcolemmal Ca^{2+} transport in streptozotocin-induced diabetic cardiopathy in rats. *Am J Physiol* **253**:E202–E207, 1987.
 32. Lagadic-Gossmann D, Buckler KJ, Prigent KL, Feuvray D. Altered Ca^{2+} handling in ventricular myocytes isolated from diabetic rats. *Am J Physiol* **270**:H1529–H1537, 1996.
 33. LaManna VR, Ferrier GR. Electrophysiological effect of insulin on normal and depressed cardiac tissues. *Am J Physiol* **240**:H636–H644, 1981.
 34. Kato M, Kako KJ. $\text{Na}^+/\text{Ca}^{2+}$ exchange of isolated sarcolemmal membrane: effects of insulin, oxidants and insulin deficiency. *Mol Cell Biochem* **83**:15–25, 1988.
 35. Tomlinson KC, Gardiner SM, Bennett T. Diabetes mellitus in Brattleboro rats: cardiovascular, fluid, and electrolyte status. *Am J Physiol* **256**:R1279–R1285, 1989.
 36. Hunter WC, Janicki JS, Weber KT, Noordergraaf A. Flow-pulse response: a new method for the characterization of ventricular mechanics. *Am J Physiol* **237**:H282–H292, 1979.
 37. Oguchi T, Kashimoto S, Yamaguchi T, Nakamura T, Kumazawa T. Is pentobarbital appropriate for basal anesthesia in the working rat heart model? *J Pharmacol Toxicol* **29**:37–43, 1993.
 38. Shimokawa A, Kunitake T, Takasaki M, Kannan H. Differential effects of anesthetics on sympathetic nerve activity and arterial baroreceptor reflex in chronically instrumented rats. *J Auton Nerv Syst* **72**:46–54, 1998.
 39. Cox RH. Three-dimensional mechanics of arterial segments in vivo methods. *J Appl Physiol* **36**:381–384, 1974.